Electrospray Ionization for Mass Spectrometry of Large Biomolecules

JOHN B. FENN, MATTHIAS MANN, CHIN KAI MENG, SHEK FU WONG, CRAIG M. WHITEHOUSE

Electrospray ionization has recently emerged as a powerful technique for producing intact ions in vacuo from large and complex species in solution. To an extent greater than has previously been possible with the more familiar "soft" ionization methods, this technique makes the power and elegance of mass spectrometric analysis applicable to the large and fragile polar molecules that play such vital roles in biological systems. The distinguishing features of electrospray spectra for large molecules are coherent sequences of peaks whose component ions are multiply charged, the ions of each peak differing by one charge from those of adjacent neighbors in the sequence. Spectra have been obtained for biopolymers including oligonucleotides and proteins, the latter having molecular weights up to 130,000, with as yet no evidence of an upper limit.

MASS SPECTROMETRY CONSISTS IN "WEIGHING" INDIVIDUAL molecules by transforming them into ions in vacuo and then measuring the response of their trajectories to electric and magnetic fields or both. Attempts to extend the sensitivity and accuracy of mass spectrometric methods to the analysis of large polar organic molecules of interest in biology and medicine have long been frustrated by the difficulties of transforming such molecules into gas-phase ions. They cannot be vaporized without extensive, even catastrophic, decomposition. Consequently, one cannot apply the classical methods of ionization that are based on gas-phase encounters of the molecule to be ionized with electrons as in electron ionization, photons as in photo ionization, other ions as in chemical ionization, or electronically excited atoms or molecules as in Penning ionization. Such encounters can remove a negatively or positively charged entity from a neutral molecule, or sometimes attach one, thus transforming it into an ion.

In the last 20 years intrepid experimentalists have developed a number of so-called "soft" ionization methods that have been used with varying degrees of success to produce intact ions from molecular species of ever-increasing size and decreasing vaporizability. One class of such methods is based on very rapid deposition of energy on a surface over which the species to be analyzed (analyte) has been dispersed. The underlying idea, first proposed by Beuhler *et al.*, is that sufficiently rapid energy input may bring about vaporization before decomposition has a chance to take place (*1*). The several methods differ in the way that rapid energy deposition is brought about. In plasma desorption (PD) it results from the impact of a fission product of a radioactive isotope, usually californium-252. So-called secondary ionization mass spectrometry (SIMS) makes use of an incident beam of high-energy ions, such as 40-keV Cs^+ and will therefore be referred to here as fast ion bombardment (FIB). If the ions are neutralized by charge exchange before they strike the surface, FIB becomes FAB (for fast atom bombardment). In laser desorption (LD), photons are the vehicle for energy deposition. These "energy-sudden" techniques have been able to produce intact ions from remarkably large analyte species, even though in an overall sense the processes involved are highly irreversible. Striking improvements have resulted from dispersing the analyte not on a bare surface but in a layer of suitable matrix, for example, thioglycerol for FAB or FIB, nitrocellulose for PD, and nicotinic acid for LD. At this writing the highest molecular weights of ions that have been produced are with LD 210,000 (*2*), with FAB (or FIB) 24,000 (*3*), and with PD 45,000 (*4*). However, product ion currents are usually very small and, except in the case of LD, decrease rapidly with increasing molecular weight of the analyte. When the ions are very large, their detection with multipliers requires postacceleration voltages that are sometimes awkwardly high. Furthermore, the ions often have high levels of internal excitation that can cause substantial peak broadening as a result of predissociation.

Quite different in practice and principle from these "violent" ionization methods are techniques that use strong electrostatic fields to extract ions from a substrate. In so-called field desorption (FD) ionization, the analyte molecules are applied to a fine wire on whose surface is disposed an array of sharp pointed needles or "whiskers." When the wire is placed in a vacuum system and a high voltage is applied while it is carefully heated, the analyte molecules desorb as ions from the tips of the needles where the field strength is very high (*5*). Even though it can transform highly nonvolatile analytes into ions in vacuo, FD has not been widely used because sample preparation is tedious. Finding and maintaining the combination of temperature and voltage that is right for a particular species requires both luck and the right touch. Finally, the desorbed ions have such high energies that relatively expensive magnetic sector analyzers must be used for their analysis. In electrohydrodynamic (EH) ionization, the analyte is dissolved in a nonvolatile liquid (for example, glycerol) and injected into an evacuated chamber through a small capillary tube that is maintained at high voltage (*6*). The

The authors are in the Chemical Engineering Department, Yale University, New Haven, CT 06520.

solvent liquid must have a low vapor pressure so that it will not "freeze-dry" from rapid evaporation into vacuum. Solute ions, along with molecules and clusters of solvent, are desorbed from the emerging liquid by the high field at its surface and can be mass-analyzed. EH, like FD, has not had many practitioners, in part because few liquids that have low vapor pressure are good solvents, in part because the desorbed ions are usually solvated with one or more molecules of the solvent, and in part because they often have a wide energy distribution. As in FD, the high ion energies in EH require magnetic sector analyzers.

Spray Ionization Methods

In the past few years a new family of ionization techniques has emerged that also make use of high electric fields to desorb ions. These techniques differ from FD and EH in that desorption is from small charged droplets of solution into an ambient bath gas instead of into vacuum. The three important members of this new family, thermospray (TS), aerospray (AS), and electrospray (ES), are all thought to share the same basic mechanism of ion production. In order to provide some perspective on this mechanism we will describe, with reference to Fig. 1, an apparatus in our laboratory that embodies ES ionization. That apparatus has been described in some detail (7). Sample solution at flow rates usually between 1 and 20 μl/min enters the ES chamber through a stainless steel hypodermic needle. The needle is maintained at a few kilovolts relative to the walls of the chamber and the surrounding cylindrical electrode that helps shape the distribution of potential and direct the flow of the bath gas. The resulting field at the needle tip charges the surface of the emerging liquid, dispersing it by Coulomb forces into a fine spray of charged droplets. Driven by the electric field, the droplets migrate toward the inlet end of the glass capillary at the end wall of the chamber. A countercurrent flow of bath gas typically at 800 torr, an initial temperature from 320 to 350 K, and a flow rate of about 100 ml/s hasten evaporation of solvent from each droplet, decreasing its diameter as it drifts toward the end wall of the chamber. Consequently, the charge density on its surface increases until the so-called Rayleigh limit is reached at which the Coulomb repulsion becomes of the same order as the surface tension. The resulting instability, sometimes called a "Coulomb explosion," tears the droplet apart, producing charged daughter droplets that also evaporate. This sequence of events repeats until the radius of curvature of a daughter droplet becomes small enough that the field due to the

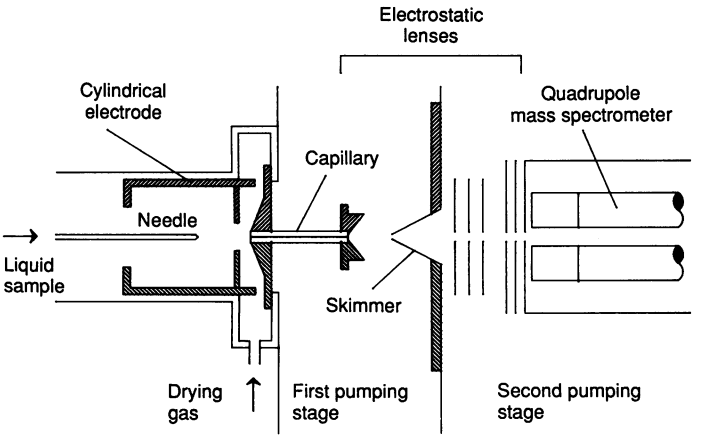

Fig. 1. Sketch of the ion desolvation process. Small, charged droplets produced by the electrospray evaporate, generating a high electric field at the droplet surface. Analyte molecules that were dissolved in the droplet can attach to charges and be lifted into the gas phase by this field.

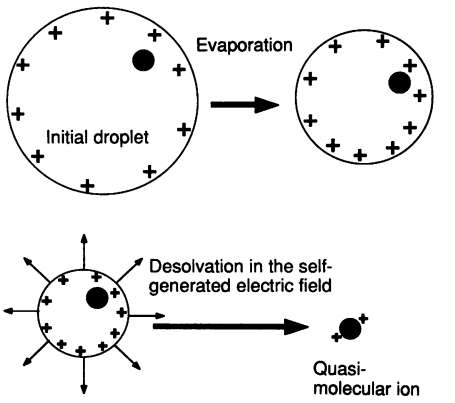

Fig. 2. Schematic diagram of an ES-MS apparatus. For details of operation, see text.

surface charge density is strong enough to desorb ions from the droplet into the ambient gas. The desorbing ions include cations (or anions), to which are attached solvent or solute species that are not themselves ions, thus producing so-called "quasi-molecular" ions suitable for mass analysis. The sequence is schematically represented in Fig. 2. This ion desorption mechanism, first proposed by Iribarne and Thomson (*8*), has certainly not been proved and indeed has been vigorously questioned by Röllgen *et al.* among others (*9*). Even so, the concept of field desorption has been a useful working hypothesis and will be assumed here even though we have some misgivings about the details of the Iribarne-Thomson model.

However they are formed, some of these ions are entrained in the flow of dry bath gas that enters the glass capillary to emerge at the exit end as a supersonic free jet in the first of two vacuum chambers. A core portion of this free jet passes through a skimmer into a second vacuum chamber, delivering ions to the analyzer, which in our present system is a quadrupole mass filter (VG Micromass 1212) with a nominal upper limit for ion mass-to-charge ratio (m/z) of 1500. The solvent vapor from the evaporating droplets along with any other uncharged material is swept away from the capillary inlet by the countercurrent flow of bath gas. Optimum values for the temperature and flow rate of the bath gas depend on the design details of a particular apparatus, the species being analyzed, and the objectives of the experiment. Flow rates that are too high may decrease sensitivity by preventing analyte ions with low mobilities from reaching the entrance to the capillary. If flow rates are too low, the extent of ion solvation may become excessive. In some cases it may be desirable for the ions to retain some solvation, in studies of cluster properties, for example, by decreasing the bath gas temperature or the flow rate. Thus, a certain amount of trial and error is advisable for determining the best flow rate and temperature for a particular experiment in a particular apparatus. Also of importance is the choice of bath gas. It should be inert in the sense of not undergoing reaction or charge exchange with analyte ions. A relatively high dielectric strength is desirable in order to avoid breakdown and discharge at the injection needle tip. If the apparatus is to run for long periods of time, the gas should be inexpensive. We have found that nitrogen is generally satisfactory. Carbon dioxide also works very well for many species and is more readily cryopumped.

The most direct way to achieve the required potential difference between the injection needle and the walls of the spray chamber is to float the sample source and the needle at the required voltage while the rest of the apparatus is at or near ground potential. The aperture leading into the vacuum system can then be a simple orifice or nozzle, as was the case in our first apparatus (*10*). When one wishes to maintain the source of sample liquid at ground potential, when the sample source is a liquid chromatograph (LC), for example, it is advantageous to replace the orifice with a capillary of dielectric

material, such as glass, as shown in Fig. 1. Satisfactory operation can then be obtained with the typical values of applied voltage shown in parentheses after each of the following components: needle (ground), surrounding cylindrical electrode (−3500 V), metalized inlet and exit ends of the glass capillary (−4500 and +40, respectively), skimmer through which a core portion of the ion-bearing gas from the free jet passes into a second vacuum chamber (−20 V), and ion lens in front of quadrupole (ground).

To produce negative ions, which are often formed by proton abstraction, similar voltages of opposite sign are applied. In addition, it is then useful to introduce a small stream of oxygen or other electron scavengers near the needle tip to inhibit the onset of a corona discharge, which occurs at lower voltages in the negative ion mode than in the positive ion mode. If the ES chamber is open to inspection any corona at the needle tip can be seen if the room is sufficiently dark and heard if it is sufficiently quiet. When the voltage is high enough to produce an incipient corona in the positive mode the adduct cation in the spectral peaks very often becomes a proton, no matter what it was at lower voltages. In the negative mode the spectra sometimes contain peaks for ions to be expected if there is a discharge in a gas containing oxygen, nitrogen, and carbon, that is, O^-, NO^-, CN^-, NO_2^-, OCN^-, and O_2^-. At corona currents much above the onset value, the effective gas conductivity becomes high enough to reduce the electric field at the needle tip and the spray becomes unstable with the formation of large droplets.

At first glance the indicated potential difference of 4540 V between the inlet and exit ends of the capillary may seem startling. We have found that with the carrier bath gas (nitrogen) at about 1 atm the ion mobility is low enough so that the gas flow through the capillary can drag the ions out of the potential well at the capillary inlet and raise them back up to ground potential or as much as 15 kV above it (*11*). Thus, we can readily provide the energies necessary for injection into a magnetic sector analyzer. The capillary, with a bore of 0.2 by 70 mm, passes just about the same flux of both bath gas and ions as did the thin-plate orifice with a diameter of 0.1 mm in our first apparatus. When a glass capillary is used as just described, the sample line along with all other external parts of the apparatus are at ground potential and pose no hazard to the operator.

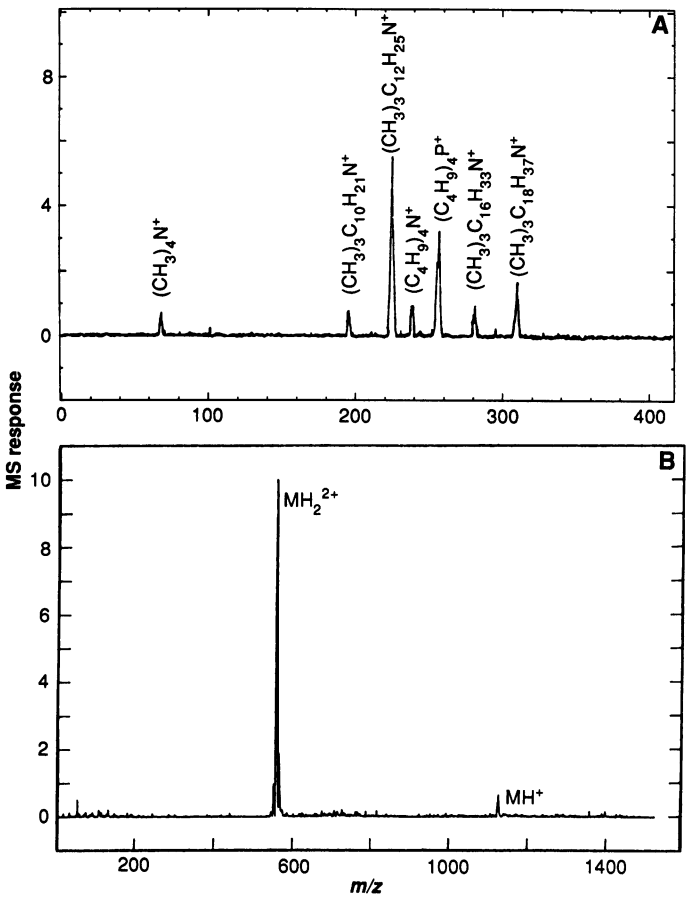

Fig. 3. (**A**) Typical electrospray spectra for nonvolatile small molecules. A mixture of quaternary ammonium and phosponium halides was dissolved at concentrations from 2 to 10 ppm in 50:50 methanol:water. (**B**) Electrospray spectrum for the peptide gramicidin S (M_r = 1141.5).

The idea of using ES dispersion of an analyte solution in a bath gas to produce solute ions for mass analysis originated with Dole *et al.* some 20 years ago (*12*). Interested in the possibility of determining the molecular weights of polymers, they performed some pioneering experiments in which an acetone-benzene solution of polystyrene macromolecules was electrosprayed into a bath gas of nitrogen in an apparatus similar to the one shown in Fig. 1. They hoped that ES dispersion of a sample solution would result in the production of ultimate droplets containing only one charge and one solute molecule. As the last solvent evaporated from such a droplet, its charge would be retained by the solute molecule, thus giving rise to a macro-ion. Because available mass analyzers could not accommodate singly charged ions with molecular weights in his range of interest, 50,000 to 500,000, Dole determined the ion kinetic energy after the skimmer by measuring the retarding potential V_r required to keep the ion from reaching a Faraday cup collector with which he measured the current I of arriving ions. Because $1/2\ m\ v^2 = z\ V_r$, where m is the mass of an ion, v is its velocity, and z is its charge, he determined m/z from values of v obtained by assuming that during the free jet expansion into vacuum the ion was accelerated to the readily calculable terminal velocity of the nitrogen bath gas. Some of his I-V_r curves showed substantial dips at values of V_r expected for singly charged ions of the macromolecules he introduced, leading him to believe that he had indeed produced singly charged ions of those macromolecules. We repeated Dole's experiments and obtained the same results. Then we both stopped further work, in part because the retarding potential method for mass analysis was troublesome. Moreover, the ion currents were very small and we had to work without the millionfold gain of ion multipliers because the large macro-ions we thought we were getting would not produce secondary electrons when they hit the first dynode of a detector unless they were accelerated to half a million volts or so (*13*).

It has become increasingly clear, for a number of reasons, that the ions detected in those early experiments could not have been singly charged macromolecules. Abundant evidence indicates that, because of slip during the expansion, their actual velocity could not have been much more than about two-thirds of the gas velocity (*14*). Nor is it likely that the ultimate droplet could have had a single charge for every molecule because the flux of molecules in the electrospray was always from 10 to 100 times that of the flux of unit charges. In addition, we have since learned that analyte molecules as large as those used in the early experiments require many attached charges in order to desorb. Moreover, they must contain polar atoms or groups to which charges can be bound by ion-dipole forces. In many recent experiments with nonpolar species, including hydrocarbons, over a wide range of sizes we have never found any evidence of ions consisting of charged single molecules. It now seems likely that what we and Dole originally saw were charged residues from the ultimate droplets, but that those residues probably comprised aggregates of polymer. Enough charges were attached so that at their actual velocity some of them had the same energy as would singly charged molecules at the jet gas velocity. Another likely problem in Dole's experiments was that his bath gas flow was concurrent with the flow

of charged droplets and ions toward the orifice in the end wall rather than countercurrent as shown in Fig. 1. It is almost certain, therefore, that there was solvent vapor in the gas entering the orifice. Ions generally make excellent condensation nuclei so that there was probably a substantial increase in the mass of any ions or charged particles due to resolvation during the adiabatic free jet expansion.

After a hiatus of some years we resumed ES experiments early in this decade. Instead of using macromolecules we started with smaller solute species, hoping to produce charged residues that would have masses within reach of an available quadrupole mass filter having an upper limit for m/z of 400. The idea was that we could learn something about the sequence of Coulomb explosions from the dependence of residue mass on flow rate and composition of injected solution. Much to our surprise, we were able to produce singly charged ions of individual solute molecules for a wide range of species (*10*). The results could not be explained by Dole's charged residue model but were entirely consistent with the ion desorption model that we described above (see Fig. 2) in the course of explaining how the apparatus in Fig. 1 worked. That model had been proposed in 1976 by Iribarne and Thomson and was supported by additional experimental results in two subsequent papers from the same group (*8*). In the experiments the droplets were produced by pneumatic atomization of sample solution and charged by statistical fluctuations in the distribution of cations and anions among the droplets. They found that currents of desorbed ions were greatly increased when an "induction electrode" was located near the nebulizing region and maintained at a potential of 3500 V. In recognition of the ion formation mechanism, Iribarne and Thomson called their ionization process "atmospheric pressure ion evaporation" (APIE). Because that same mechanism also seems to apply to the other two members of the family, ES, which has already been described, and TS, which will be described shortly, we will refer to APIE as aerospray (AS) in recognition of the aerodynamic forces used to atomize the sample liquid.

Thermospray (TS) was developed by Vestal and his colleagues starting about the beginning of the decade (*15*). Although it was the last to arrive on the scene, TS is by far the most widely used of the spray techniques and has become a well-known and effective interface between a liquid chromatograph and a mass spectrometer in so-called LC-MS. The sample solution is passed through a capillary tube whose walls are at a temperature high enough to vaporize 90 to 95% of the solvent. The shear and acceleration forces resulting from the expansion atomize the remaining liquid so that a mixture of droplets in vapor issues from the end of the tube as a supersonic jet into a region with walls hot enough to maintain the vapor in a superheated state so that the droplets can evaporate. They are charged, positively and negatively in equal numbers, by the same statistical fluctuations that produce charging in AS when there is no induction electrode. In a sequence of steps probably similar to those in ES and AS, ions are produced by desorption from the evaporating droplets and pass into a vacuum system for analysis. In TS and AS (especially without an induction electrode) the droplet-charging results from atomization of the liquid. In ES, which can be considered a sort of mirror image of TS and AS, atomization of the liquid results from charging. This operational difference is important because it results in much higher droplet charge-to-mass ratios for ES than for TS or AS, with consequent substantial increases in analytical sensitivity. For the same reason ES can produce ions with far more extensive multiple charging than can be obtained by TS, AS, or any other method yet developed. This multiple charging capability is of profound importance.

In this discussion AS refers to the embodiment found most successful by Thomson and Iribarne in which the presence of an induction electrode means that both electrostatic and aerodynamic forces were used in nebulizing the sample liquid. Other combinations of electrostatic, pneumatic, and thermal forces have been explored. The most recent of these, so-called "Ionspray," was introduced by Henion and his colleagues and this name has now been adopted as a trademark by one supplier of mass spectrometers (*16*). It features an annular flow of gas around the liquid emerging from an injection needle at high voltage. Although it does allow higher liquid flow rates than can be used with pure ES, as claimed, this same configuration was tried nearly 20 years ago by Dole and discarded because it produced lower ion currents than unassisted ES. Reflection suggests that any such attempt to "assist" ES dispersion of sample liquid must inevitably lower the ratio of charge to mass in the resulting droplets and therefore decrease analytical sensitivity because, to a first approximation, ES current is independent of flow rate. Indeed, the best results reported with Ionspray are always obtained at low liquid flow rates, well within the range that pure ES can accommodate without any help. It seems clear that a more attractive solution to the problem of a large sample flow might be to split the flow and carry out unassisted ES-MS analysis on a small side stream, leaving the bulk of the main stream available for other purposes or additional analysis.

Electrospray Mass Spectra

The analyzer in our first bona fide ES-MS experiments was a quadrupole mass filter with a nominal upper limit of 400 for the molecular weight of the ions it could accommodate. With it we were able to obtain ions from almost any solute species within its mass range, so long as that species incorporated a polar atom or group (*10*). Figure 3A shows a spectrum obtained with a solution containing a few parts per million of one quaternary phosponium halide along with several quaternary ammonium halides. None of these compounds can be vaporized without decomposition but the ES spectrum shows no evidence of either fragmentation or interference between species.

Among the first substances we studied with the "new" apparatus of Fig. 1 was the cyclic decapeptide gramicidin S, whose ES spectrum is presented in Fig. 3B. It shows peaks corresponding to the singly and doubly charged parent. The relative intensities of

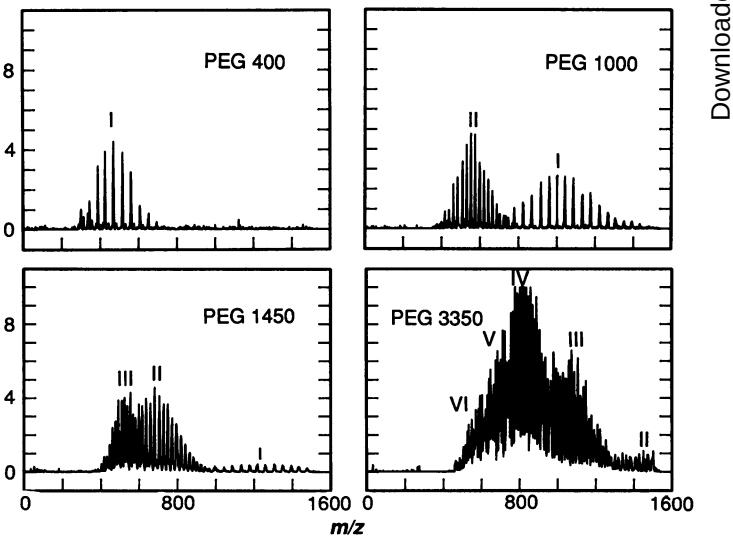

Fig. 4. Electrospray spectra for PEG samples of varying molecular weight in a methanol-water mixture. The nominal molecular weight refers to the most abundant oligomer.

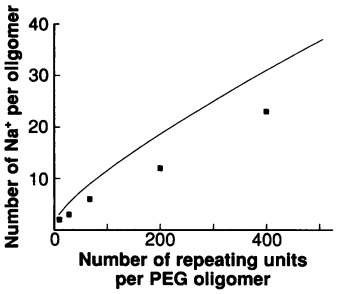

Fig. 5. Dependence of the number of charges (Na^+) per oligomer of PEG on the number of constituent monomers. The solid curve shows what the model predicts, and the squares are from measured spectra.

these peaks are strongly dependent on solution composition as well as analyte concentration. The doubly charged peak becomes predominant and the singly charged peak almost vanishes at very low concentration. The relative magnitudes of singly and doubly charged peaks also depend on structure. At concentrations for which cyclosporin A, a peptide of similar size, produces only singly charged ions, gramicidin S produces mostly doubly charged ions. The slightly smaller bradykinin shows a strong, triply charged peak. This behavior is consistent with the fact that gramicidin S has two basic amino acids in its ring and that bradykinin has basic residues at both ends of its sequence.

We were intrigued by these observations of multiple changing because the effective mass range of any analyzer is increased by a factor equal to the number of charges on an ion. Accordingly, we undertook a study of ES ions produced from poly(ethylene glycols) (PEGs) (*17*). These PEGs are attractive species for such a study because their chemical structure is essentially independent of size. The component monomers of these polymers are ethylene oxide, whose molecular weight is 44. They are readily available over a wide range of molecular weights that ranged in our experiments from 400 to 17,500. These nominal values relate to the mass of the most abundant oligomer in a Gaussian distribution whose full width at half height is about 30% of the nominal value. The spectra in Fig. 4 comprise bands of peaks with a Gaussian intensity distribution. Each peak corresponds to an oligomer whose component monomers differ in number by one from peak to adjacent peak. The adduct charges are Na^+ ions resulting from the presence of sodium in the samples. A similar distribution of much smaller peaks for ions in which the adduct charge is K^+ can be distinguished in the original spectrum.

From the spacing between the peaks it is easy to arrive at the number of charges, indicated by the Roman numerals. Both the congestion and the jaggedness of the profile in a band increase as the nominal molecular weight of the PEG sample and the number of charges per oligomer increase. These effects stem from the associated increase in the number of possible combinations of oligomer mass and charge, which lead to increasing congestion and superposition of peaks too close together on the *m/z* scale to be resolved by our analyzer, which had an effective resolution of about 300. For PEG 8,000 and PEG 17,500 the spectral congestion is such that there are as many as six or seven peaks per unit interval in *m/z*, so that the spectra include bands with nearly continuous but noisy-looking profiles. In spite of this lack of resolution, by assuming that the *m/z* value of the profile peak corresponds to the most abundant oligomer, we arrive at values of 10 and 23, respectively, for the average number of charges per oligomer of PEG 8,000 and PEG 17,500.

We can estimate the maximum number of charges that an oligomer can retain on the basis of a simple model in which the electrostatic repulsive energy of a charge is calculated from a pairwise addition of its Coulomb interactions with all other charges on an oligomer. A charge can be retained by the oligomer only if its repulsion energy is less than the attractive energy of the bond between the charge and the oxygen atom to which it tries to attach. The ordinate values for the solid curve in Fig. 5 show the maximum number of charges calculated by this model for an oligomer containing the number of constituent monomers indicated on the abscissa. The points are experimental values. Clearly the model allows more charges per oligomer than are found in the experiment. Part of the discrepancy may be due to factors that the model ignores. For example, fluctuations in oligomer configuration due to Brownian motion may result in an average distance between oxygen atoms that is less than the assumed distance, which was based on a stretched linear configuration. However, we think it more likely that the explanation is kinetic rather than thermodynamic. Ions may desorb before they have a chance to collect all the charges the model would allow them to retain.

These PEG results demonstrated the ability of ES to produce multiply charged intact ions from relatively large parent species. Even so, the response in the community of mass spectrometrists was somewhat muted until the first results with proteins were revealed (*18*). Figure 6 shows four representative mass spectra for species with molecular weights from 5,000 to 76,000. Samples were dissolved in solvents comprising mixtures of acetonitrile, water, and methanol or 1-propanol. For these particular analytes it was advantageous to lower the solution *p*H by the addition of small quantities

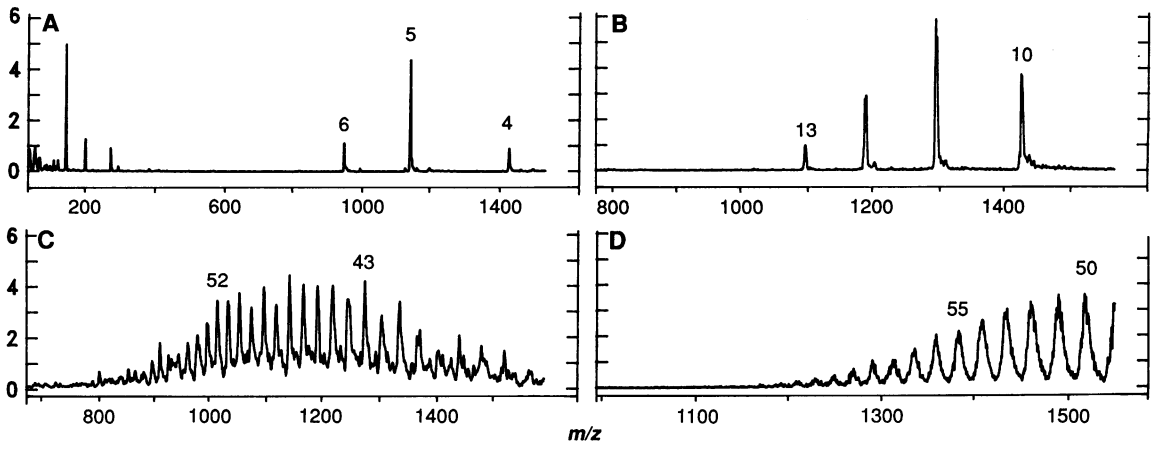

Fig. 6. Representative electrospray mass spectra for protein samples in acidified mixtures of water and methanol. The adduct ions were protons, and the solution flow rate was 1 or 2 μl/min. The spectra are the results of single, 30-s scans. Approximate molecular weight and amount of samples used in the spectrum are as follows: (**A**) insulin, 5,730, 1.7 pmol; (**B**) lysozyme, 14,300, 175 fmol; (**C**) α-anylase, 54,700, 1.7 pmol; and (**D**) conalbumin, 76,000, 200 fmol. See Table 1 for more data.

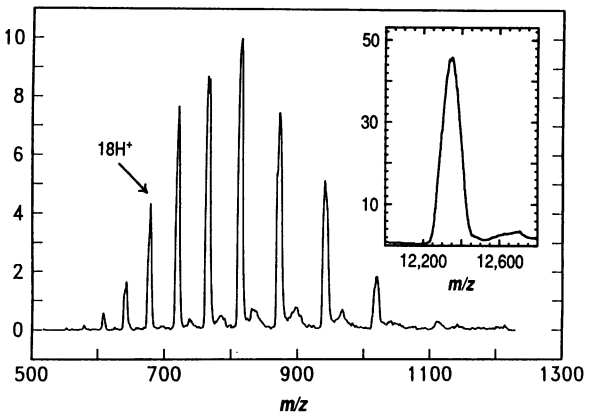

Fig. 7. Application of the "deconvolution algorithm" to a measured spectrum of cytochrome c. The insert shows the deconvoluted peak resulting from the transformation. Intensities of the measured and deconvoluted spectra are to the same scale.

of acetic acid or trifluoroacetic acid. The optimum proportions of these solvent components depended somewhat on the particular sample and were determined by trial and error. Solutions with analyte concentrations ranging from 0.22 to 137 μmol/liter, depending on the species, were injected at flow rates between 1 and 8 μl/min. We have been able to obtain complete spectra with a few femtomoles of material. We have not yet mounted an effort to push the limits of sensitivity but in general it increases with decreasing flow rate because total ES current does not depend appreciably on flow rate so that the ratio of available charge to analyte mass increases as flow rate decreases. Each of the spectra shown is the result of a single scan requiring 30 s to cover the indicated mass range. This scan speed is as fast as can be accommodated by our homemade data-processing system based on an IBM-AT clone. Oscilloscope inspection during faster scan speeds suggests that we could obtain similar signal-to-noise ratios in scans lasting only 3 s.

Essential features of the spectra in Fig. 6 are summarized in Table 1 along with equivalent data from several other proteins. For a single substance each spectrum comprises a sequence of peaks that are coherent in the sense that the component ions of each peak differ from those of the immediately adjacent peaks by a single adduct charge, which in the case of proteins is almost always a proton. The envelopes of the peaks have shapes that are nearly Gaussian and occupy a "window of desorbability" with upper and lower limits that vary somewhat but nearly always fall completely within the nominal m/z range of our analyzer, 0 to 1500. For the exceptions the upper limit of this window would still seem to be less than 3000 or so. None of the more recent experiments suggest that it will be appreciably higher for any species. This upper limit of m/z for desorption can be attributed to the requirement that a molecule attach some minimum number of charges to overcome solvation forces and achieve "lift-off." Because solvation forces per unit length (mass) of molecule should not be that different for most species, the upper value of m/z in a spectrum should always lie within a modest range of values. Similarly, the lower limit of the m/z desorption window can be understood in terms of a rapid decrease in desorption time as the number of charges per unit length of molecule increases. As we suggested might be the case for PEG, when a molecule collects some limited number of charges per unit length, it desorbs before it can garner any more.

There is no evidence of fragmentation in the ES spectra for these large species. However, for proteins having subunits that are not covalently bonded to the rest of the molecule, for example, hemoglobin, ion masses correspond to these subunits rather than to the complete protein. This observation is in agreement with our model

Table 1. Data for the spectra in Fig. 6 and corresponding data for several other proteins. The molecular weight given was determined from the sequence and is the chemical molecular weight M_r, that is, the average value based on the natural abundance of isotopes. α-Amylase and conalbumin masses are from the spectra in Fig. 6.

Compound	Molecular weight	Concentration		Range of	
		μg/μl	μmol/liter	Charges	m/z
Insulin (bovine)	5,730	0.01	1.7	4–6	950–1450
Cytochrome c (horse heart)	12,400	1.67	135	12–21	550–1100
Lysozyme (chicken egg)	14,300	0.005	0.35	10–13	1100–>1500
Myoglobin (equine skeletal muscle)	17,000	0.50	29.5	16–27	600–1100
α-Chymotrypsinogen A (bovine pancreas)	25,700	0.50	19.0	17–22	1150–>1500
Alcohol dehydrogenase (horse liver)	39,800	0.50	12.5	32–46	800–1300
α-Amylase (bacterial)	54,700	0.1	1.8	35–58	880–1550
Conalbumin (chicken egg)	76,000	0.017	0.22	49–64	1200–>1500

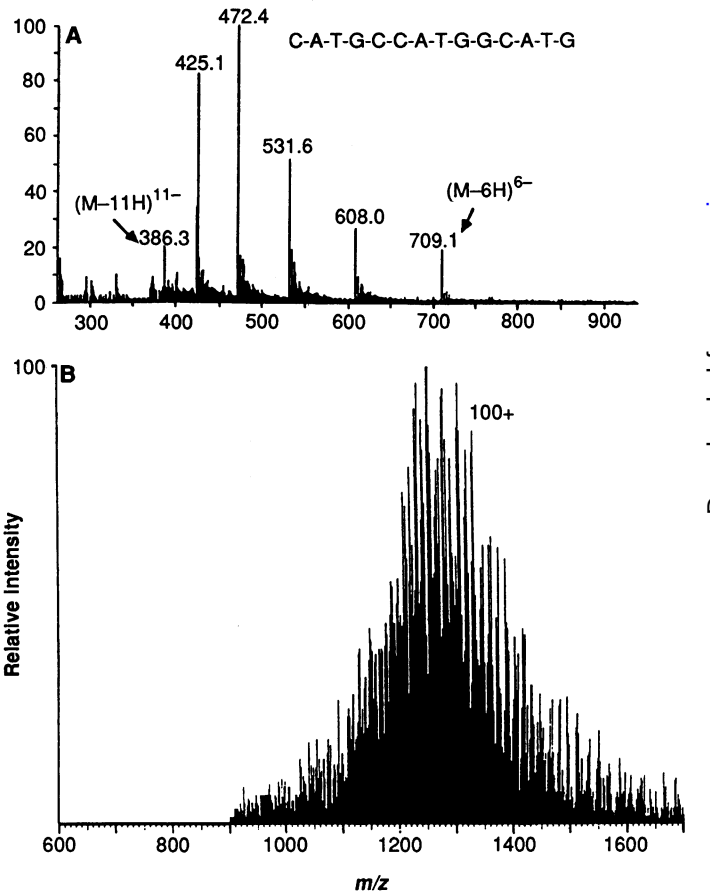

Fig. 8. Electrospray mass spectra for large molecules obtained by other investigators: (**A**) for a synthetic oligonucleotide (*21*); (**B**) for a larger protein, bovine albumin dimer (molecular weight, 133,000) (*23*). [Adapted from (*21*) with permission of the authors and the editor of *Rapid Communications in Mass Spectrometry*]

for charging that assumes a "stretching-out" of the configuration that might lead to separation of subunits that are only loosely bound. The model is also consistent with the observation that, in general, the centroid of the distribution of multiply charged ions shifts to higher values on the *m/z* scale as the number of disulfide bonds of the protein increases. (A protein with disulfide bonds cannot stretch into a linear configuration.) For example, myoglobin has a molecular weight of 17,000 and no disulfide bonds, whereas α-chymotrypsinogen A has a molecular weight of 25,600 and five disulfide bonds. Under similar experimental conditions, myoglobin can maximally hold 27 charges whereas α-chymotrypsinogen A can hold only 22 charges even though it is half again as large (in terms of mass)(*19*).

There is a most important consequence of the peak multiplicity in these ES spectra. There are three unknowns associated with each peak: the mass of the parent molecule, the number of adduct charges, and the mass of each such charge. Because of the coherence of the peak sequence, which is quantized in the sense that ions of adjacent peaks differ by only one adduct charge, it is easy to arrive at the number of charges on the ions of each peak. Because the choices available for adduct ions are usually limited to such species as H^+, NH_4^+, Na^+, and K^+, which have relatively large mass differences, it is similarly easy to obtain a good estimate for the adduct mass. Consequently, each peak constitutes an independent measure of the mass of the parent species so that signal-averaging can be carried out with a single spectrum. As a result, mass assignment can be made with greater precision and more confidence than is possible with spectra of singly charged ions. This averaging possibility has been described in detail elsewhere (*20*). Thus, for example, if a spectrum has ten resolved peaks, an averaged mass assignment can be made with an uncertainty more than $\sqrt{10}$ times smaller than would be the case for one peak. Also described in (*20*) is a "deconvolution algorithm" that transforms the multiplicity of peaks into the single peak that would be expected if all the ions had a single charge. Figure 7 illustrates the result of applying this algorithm to a measured cytochrome c spectrum.

Prospectus

Interest in ES ionization seems to have exploded after some of these protein results were presented at the 36th American Society for Mass Spectrometry (ASMS) Conference on Mass Spectrometry and Allied Topics at San Francisco in June 1988. Within a few months Covey *et al.* had confirmed our results and with the spectrum shown in Fig. 8A demonstrated that ES worked just as well with oligonucleotides in the negative ion mode (*21*). Meanwhile, Smith and his colleagues, who have pioneered the coupling of capillary zone electrophoresis to ES (*22*), confirmed our expectations with the spectrum in Fig. 8B. It demonstrates that ES ionization makes possible the mass analysis of proteins with molecular weights up to at least 130,000 (*23*). One year later, at the 37th ASMS Conference in Miami, there was a great profusion of communications on ES ionization. The Covey and Smith groups reported some very exciting developments in the MS-MS analysis of proteins with a triple quadrupole analyzer and ES ionization. In spite of their very large masses, these multiply charged ions can be readily dissociated by gas-phase collisions with argon or helium. The implications for the sequencing of biopolymers are enormous and present many challenging opportunities for further research.

As a final portent of things to come, we show the spectrum in Fig. 9 presented at that 37th ASMS Conference by McLafferty and his colleagues (*24*). It was obtained with multiply charged ions from an external ES source mass-analyzed by means of Fourier transform ion cyclotron resonance (FTICR). This technique has long promised to offer the ultimate in resolution for mass analysis but has had inherent difficulties with heavy ions because of the low frequency of their cyclotron orbits. The multiple charging of ES brings the *m/z* values of very large ions well within a range for which FTICR is well suited. This marriage of ES with FTICR to provide very high resolution in the analysis of very large ions promises to be a fruitful union.

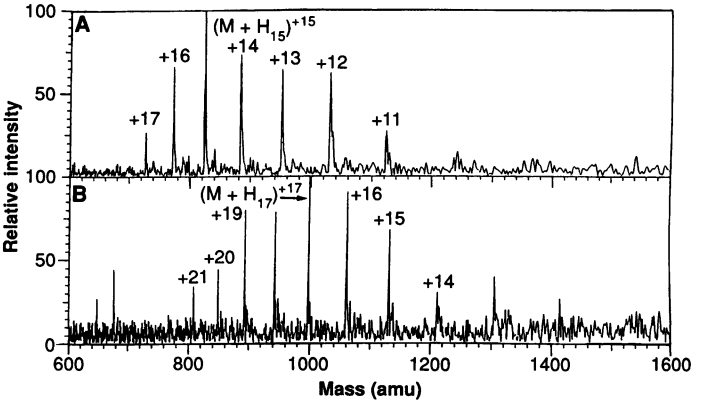

Fig. 9. Electrospray mass spectra obtained by coupling an ES source to a Fourier transform mass spectrometer (*24*): (**A**) cytochrome c (equine); calculated average molecular weight, 12,360.1; measured molecular weight, 12,356.9 ± 0.9; (**B**) myoglobin (equine skeletal muscle); calculated average molecular weight, 16,950.7; measured molecular weight, 16,947.5 ± 1.4.

REFERENCES AND NOTES

1. R. J. Beuhler, E. Flanigan, L. J. Green, L. Friedman, *J. Am. Chem. Soc.* **96**, 3990 (1974).
2. M. Karas and F. Hillenkamp, *Anal. Chem.* **60**, 2299 (1988); paper presented at the 11th International Mass Spectrometry Conference, Bordeaux, France, 1988, and American Society for Mass Spectrometry (ASMS) Workshop on Ion Desorption Mechanisms, Sanibel Island, FL, January 1989.
3. M. Barber and B. N. Green, *Rapid Commun. Mass Spectrom.* **1**, 80 (1987).
4. G. Jonsson *et al.*, *ibid.* **3**, 190 (1989).
5. H. D. Beckey, *Principles of Field Ionization and Field Desorption Mass Spectrometry* (Pergamon, Oxford, 1977).
6. D. S. Simons, B. N. Colby, C. A. Evans, Jr., *Int. J. Mass Spectrom. Ion Phys.* **15**, 291 (1974); K. D. Cook, *Mass Spectrom. Rev.* **5**, 467 (1986).
7. C. M. Whitehouse, R. N. Dreyer, M. Yamashita, J. B. Fenn, *Anal. Chem.* **57**, 675 (1985).
8. J. V. Iribarne and B. A. Thomson, *J. Chem. Phys.* **64**, 2287 (1976); B. A. Thomson and J. V. Iribarne, *ibid.* **71**, 4451 (1979); J. V. Iribarne, P. J. Dziedzic, B. A. Thomson, *Int. J. Mass Spectrom. Ion Phys.* **50**, 331 (1983).
9. F. W. Röllgen, E. Bramer-Wegner, L. Bütfering, *J. Phys.* **48**, C6-253 (1987); M. Vestal, in *Ion Formation from Organic Solids*, A. Benninghoven, Ed. [*Springer Ser. Chem. Phys.* **25**, 246 (1983)].
10. M. Yamashita and J. B. Fenn, *J. Phys. Chem.* **88**, 4451 (1984); *ibid.*, p. 4471.
11. C. M. Whitehouse, M. Yamashita, C. K. Meng, J. B. Fenn, in *Proceedings of the 14th International Symposium on Rarefied Gas Dynamics*, H. Oguchi, Ed. (Univ. of Tokyo Press, Tokyo, 1985), pp. 857–864.
12. M. Dole, L. L. Mach, R. L. Hines, R. C. Mobley, L. P. Ferguson, M. B. Alice, *J. Chem. Phys.* **49**, 2240 (1968); L. L. Mach, P. Kralik, A. Rheude, M. Dole, *ibid.* **52**, 4977 (1970); G. A. Clegg and M. Dole, *Biopolymers* **10**, 821 (1971); D. Teer and M. Dole, *J. Polym. Sci.* **13**, 985 (1975).
13. R. J. Beuhler and L. Friedman, *Nucl. Instrum. Methods* **170**, 309 (1980).
14. N. Abuaf, J. B. Anderson, R. P. Andres, J. B. Fenn, D. R. Miller, in *Rarefied Gas Dynamics*, C. L. Brundin, Ed. (Academic Press, New York, 1967), vol. 2, pp. 1317–1336; J. B. Anderson, *Entropie* **18**, 33 (1976).
15. C. R. Blakley, M. J. McAdams, M. L. Vestal, *J. Chromatogr.* **158**, 264 (1978); C. R. Blakley, J. J. Carmody, M. L. Vestal, *Anal. Chem.* **52**, 1636 (1980); *Clin. Chem.* **26**, 1467 (1980); *J. Am. Chem. Soc.* **102**, 5931 (1980); M. L. Vestal, in *Mass Spectrometry in the Health and Life Sciences*, A. L. Burlingame and N. Castagnoli, Jr., Eds. (Elsevier, Amsterdam, 1985), pp. 99–118.
16. A. D. Bruins, L. O. G. Weidolf, J. D. Henion, *Anal. Chem.* **59**, 2647 (1987).
17. S. F. Wong, C. K. Meng, J. B. Fenn, *J. Phys. Chem.* **92**, 546 (1988).
18. C. K. Meng, M. Mann, J. B. Fenn, *Z. Phys. D* **10**, 361 (1988); M. Mann, C. K. Meng, J. B. Fenn, in *Proceedings of the 36th Annual Conference on Mass Spectrometry and Allied Topics* (San Francisco, CA, June 1988) (ASMS, East Lansing, MI, 1988), p. 771.

19. M. Mann, thesis, Yale University (University Microfilms) (1989).
20. ———, C. K. Meng, J. B. Fenn, *Anal. Chem.* **61**, 1702 (1989); in *Proceedings of the 36th Annual Conference on Mass Spectrometry and Allied Topics* (San Francisco, CA, June 1988) (ASMS, East Lansing, MI, 1988), p. 1207.
21. T. R. Covey, R. F. Bonner, B. I. Shushan, J. D. Henion, *Rapid Commun. Mass Spectrom.* **2**, 249 (1988).
22. J. A. Olivares, N. T. Nhung, C. L. R. Yonker, R. D. Smith, *Anal. Chem.* **59**, 1230 (1987); R. D. Smith, J. A. Olivares, N. F. Nguyen, H. R. Udseth, *ibid.* **60**, 436 (1988).
23. R. D. Smith, J. A. Loo, C. J. Barinaga, H. Udseth, paper presented at the 5th (Montreux) Symposium on LC-MS, Freidburg, November 1988.
24. F. W. McLafferty *et al.*, paper presented at the 37th Annual Conference on Mass Spectrometry and Allied Topics (Miami, FL, May 1989).
25. Early exploratory work that led to the developments described here was sponsored in part by the Department of Energy and in part by the National Science Foundation. Funding for most of the work since has been provided by the National Institutes of Health with some assistance from the donors of the Petroleum Research Fund. Continuity of effort between these early and later phases of our research was made possible by a grant from the American Cancer Society. We are grateful for the interest and many stimulating discussions provided by friends and colleagues too numerous to identify here.

Some Developments in Nuclear Magnetic Resonance of Solids

B. F. Chmelka and A. Pines

Nuclear magnetic resonance (NMR) spectroscopy continues to evolve as a primary technique in the study of solids. This review briefly describes some developments in modern NMR that demonstrate its exciting potential as an analytical tool in fields as diverse as physics, chemistry, biology, geology, and materials science. Topics covered include motional narrowing by sample reorientation, multiple-quantum and overtone spectroscopy, probing porous solids with guest atoms and molecules, two-dimensional NMR studies of chemical exchange and spin diffusion, experiments at extreme temperatures, NMR imaging of solid materials, and low-frequency and zero-field magnetic resonance. These developments permit increasingly complex structural and dynamical behavior to be probed at a molecular level and thus add to our understanding of macroscopic properties of materials.

Nuclear magnetic resonance (NMR) involves the absorption and emission of radio-frequency energy by nuclear spins as they oscillate and reorient in the presence of internal and externally applied magnetic fields. The oscillation frequencies and reorientation times depend sensitively on the local environments and on the mobility of the atoms and molecules. The sensitivity of the resulting spectrum to local environment in the sample, together with a natural isotopic selectivity, enables NMR to provide detailed information about structure and dynamics for many classes of materials (*1–4*).

The interactions that determine an NMR spectrum depend, in general, on the microscopic orientation of the atomic or molecular species in a magnetic field. For molecules randomly oriented in a rigid lattice, the variety of possible orientations often leads to a correspondingly complicated spectrum. In liquids, by contrast, the rapid and isotropic molecular motion averages the anisotropic interactions and thus narrows the spectral lines. The study of solids is therefore complicated because line broadening and low sensitivity frequently obscure the spectral features from which structural and dynamical details are to be extracted. Development of new instrumentation and analytical techniques that produce better resolved and more detailed spectra, however, continues to expand the application of NMR in various fields such as physics, chemistry, biology, medicine, geology, and materials science. In this review we describe a few recent developments in NMR (with selected references from the most recent literature) that demonstrate its exciting analytical potential in the study of solids. While the selection of topics and references is by no means comprehensive (or even democratic), we hope that it illustrates some of the novelty and diversity of modern NMR.

The authors are at the Lawrence Berkeley Laboratory and the University of California, Berkeley, CA 94720.

Line-Narrowing by Sample Reorientation

One way to narrow the broad lines in the NMR spectrum of a solid is to reorient the sample rapidly to average away the anisotropic effects artificially. Methods of this sort seek to resolve spectral details from which individual atomic sites can be identified and internuclear distances determined. Magic-angle spinning (MAS), in which a sample is rotated about an axis inclined at 54.7° (the "magic angle") with respect to the magnetic field, has been widely used, particularly for spin-½ nuclei such as ^{13}C, ^{15}N, ^{19}F, ^{29}Si, and ^{31}P, to diminish the broadening effects of chemical shift anisotropy and magnetic dipole-dipole coupling. High resolution spectra in complex solids have been obtained recently for ^{13}C in biopolymers (*5*), for ^{29}Si in a zeolite (Fig. 1) (*6*), and for ^{15}N in a protein (Fig. 2) (*7*), for example. Some recent advances in this area include development of fast MAS (with spinning speeds in excess of 20 kHz) (*8*), MAS in combination with multiple-pulse NMR (*9*), MAS with rotational resonance (*10*), and MAS with double resonance echoes (*8*). High-resolution structural information provided by NMR is generally short range in nature, and serves to complement the longer range periodicity to which diffraction techniques are sensitive. The ability to resolve structure over short distances is especially important for